Preparation and evaluation of bacillus thuringiensis microcapsules based on biochar

B. H. Zhang[a], L. L. Xin[a], H. Y. Zhu[c], G. Y. Yan[a], C. Y. Li[b,*]

[a]*Institute of New Pesticide Innovation and Research, Qingdao Agricultural University, Qingdao 266103, People's Republic of China*
[b]*Key Lab of Integrated Crop Pest Management of Shandong Province, College of Plant Health and Medicine, Qingdao Agricultural University, Qingdao 266109, P eople's Republic of China*
[c]*College of Energy and Chemical Engineering, Ningxia Vocational Technical College of Industry and Commerce, Yinchuan,750021, People's Republic of China*

The walnut shell biochar was prepared at high temperature in this experiment. The effect of different biochar on the growth of *Bacillus thuringiensis* (Bt) were investigated, and biochar with good biocompatibility to Bt was selected and used as an adsorbent to prepare Bt/ sodium alginate/ biochar composite microspheres. The effects of sodium alginate, calcium chloride mass fraction, and biochar addition on the encapsulation rate and the spheroidization rate of microspheres were investigated. The results showed that the optimum preparation conditions were as follows: the mass fractions (w/v) of sodium alginate, biochar, and calcium chloride were 3%, 0.4%, and 2%, respectively. The encapsulation rate and sphericity rate of prepared composite microspheres were 93.50% and 90%, and the diameter was about 1200 μm after drying. Release behavior in water showed that Bt-sodium alginate-biochar microspheres had better sustained release performance than those without biochar.

1. Introduction

Biochar is a pyrolysis product of organic matter pyrolyzed at high temperature and low oxygen content [1], and it generally has aromatic hydrocarbons and a tubular structure similar to graphene. In recent years, it has attracted extensive attention from scholars at home and abroad as a slow-release carrier for fertilizers, soil amendment, pollutant remediation, carbon emission reduction, and other aspects [2]. Due to the developed porosity and large specific surface area of biochar, it has a good adsorption effect, and high cation exchange capacity (CEC) performance [3], which can be used as an excellent functional microbial carrier [4-6] to achieve the purpose of cell or microbial immobilization and culture. By immobilizing microbial cells, the microorganisms are protected, thereby preventing the bacteria from being affected by toxic compounds, making the treatment process easy to control, and the cell loss is reduced, while the conventional immobilization techniques (such as sodium alginate immobilization technology) have microbial

---

* Corresponding author: cyli@qau.edu.cn

cells and matrix. Defects such as large diffusion resistance, loss of cell activity, and poor mechanical strength [7]. There have been many reports on the use of biochar fixed degrading bacteria to achieve continuous degradation of environmental pollutants [8-10]. However, there are few reports on the use of biochar to immobilize microbial pesticides to achieve the controlled release of pesticides.

Bacillus thuringiensis (Bt) is a widely used microorganism insecticide that is the world's most studied and harmless to humans and livestock and does not destroy the ecological balance [11]. In 1992, Ohba isolated and screened a new Bt strain Buibui with specific insecticidal activity to scarab larvae [12], which aroused great interest and concern and in the use of Bt to control grubs. At present, more than 30 strains of Bt with insecticidal activity against grubs have been isolated at home and abroad [13]. Li Changyou isolated a new Bt strain B-Y7-1 with high insecticidal activity against *Holotrichia oblita* and *Holotrichia parallela Motschulsky* [14]. The main insecticidal components of Bt are spores, crystal proteins, and other active substances. The shortcomings such as short duration of efficacy, easy to be restricted by external climate, and ecological conditions such as sunshine, temperature, and rainwater [15], which results in a short duration of field application of Bt. Therefore, the technology of encapsulating Bt with microcapsules and microspheres emerged. He Xiaolin prepared biocompatible microcapsules of Bt crystals targeted for control of Lepidoptera larvae [16]. Josefina used the emulsion internal gelation method to produce microcapsules of Bt [17]. Experiments show that the microencapsulated Bt enhanced the resistance to ultraviolet, temperature, and other adverse environments, and protected the active substances of Bt.

In this study, biochars were prepared from walnut shell at different pyrolysis temperatures. The biocompatibility of different biochars with Bt was also investigated. On this basis, biochar/sodium alginate sustained-release microspheres loading Bt were prepared. The optimal preparation conditions were obtained by determining the influence of different factors on the properties of the microspheres. The structure of Bt microspheres was characterized by SEM, and the release behavior of Bt from the microspheres was evaluated.

2. Materials and methods

2.1. Bacterial strain and medium

Bacillus thuringiensis B-Y7-1 (Bt) was isolated from soil (Shandong, China) by the research center of the invertebrate cell. The strain was cultivated at 30 ± 1°C, 120 rpm in fresh sterilized Luria-Bertani (LB) medium consisting of 1% tryptone (Qingdao Hope Bio-Technology Co., Ltd), 0.5 % yeast extract (Beijing Land Bridge Technology Co., Ltd.), and 1 % NaCl (China Pharmaceutical Group Chemical Reagents Co., Ltd.) for approximately 48 h. All Bt cultures were collected by centrifugation at 8,000 rpm for 15 min without washing. The cultured were stored in deionized water at 4°C.

2.2. Preparation of biochar

Walnut shell is the feedstocks of biochar, came from the same batch of purchases in shopping malls (Shandong, China), and were pulverized by universal highspeed smashing machines. The pulverized walnut shell was passed through a 2 mm sieve and dried in a drying

oven at 80 ℃ for 4 h. Then, it is divided into mash, compacted, sealed, placed in a muffle furnace, and raised to a carbonization temperature of 400 ℃, 500 ℃, 600 ℃ at a temperature of 10 ℃/min under high vacuum for 6 h [18], and were marked H-4, H-5, and H-6, respectively.

2.3. Physicochemical properties of biochar

pH: Take 2.00 g biochar sample, add 40.00 g deionized water, shake for 1 h, and stand for 10 minutes, then determine its pH value.

Yield (Y%): The yield of biochar refers to the difference between the mass of the material before carbonization (M0) and the mass of the material after carbonization (M1) [19]. as defined as the following expression (1).

$$Y(\%) = \frac{M_1}{M_0} \times 100 \tag{1}$$

Ash content: Biochar samples of about 2.0 g were dried at 105 ℃ and weighed. The dried samples were put into a muffle oven and burned at 750 ℃ for 6 hours. When the muffle oven was cooled to 300 ℃ left, the samples were put into a dryer and weighed after cooling. Repeat the above steps until the weight change of the sample is less than 0.0005 g. Calculate the ash content of the biochar according to the weight change [20].

2.4. Characterization of biochar

The FTIR characteristic peaks of the different processed walnut shell biochars were determined by Fourier transform infrared spectroscopy (Varian 640-IR , China.). The morphology and structure of biochar were observed by SEM (JEOL7500F, Japan).

2.5. Effect of biochar on the biocompatibility of Bt

Biochar (H-4, H-5 and H-6) was added into 150 mL flask containing 50 mL LB solid medium (1.3 g LB + 1.0 g agar) in a certain proportion (W/V): 0.5 %, 1 %, 1.5 %, 2 % and 2.5 %. The LB medium to which no biochar was added was used as a control, and it was recorded as CK. The medium was sterilized at 121 ℃ for 30 min, poured into petri dishes, and Bt was added. Incubate at 30 ℃ for 48 h, and measure the diameter of the cake by the cross method, which is compared with CK.

2.6. Preparation of microspheres

The controlled release system was prepared with Bt as a model drug (bacteria) and sodium alginate as wall material. The effects of biochar addition amount, sodium alginate concentration, and $CaCl_2$ concentration on the entrapment rate and balling rate of Bt in microspheres were investigated. Bt bacterial solution was added into the mixed solution of sodium alginate and biochar, and the mixed solution was dripped into the calcium chloride solution by 2.5 mL syringe. Bt/sodium alginate/biochar microspheres were prepared by solidification for 30 minutes, filtration, washing with sterile water twice, and drying.

Embedding rate (EE%): Bt suspension was diluted and cultured in the PCA medium. The number of colonies was counted as N_0. The microspheres prepared with the same amount of Bt were added into the sodium citrate solution with a proper concentration of 3.8 % (w/v) after sterilization. The microspheres were broken and dissolved by ultrasound for 10 min. The clear

solution was counted and cultured in the PCA medium and recorded as N_1. The embedding rate was calculated as defined as the expression (2).

$$EE(\%) = \frac{N_1}{N_0 \times \text{dilution times}} \times 100 \tag{2}$$

Granulation rate (GR%): The ratio of the number of regular microspheres (N_2) formed by 1 mL of the sample solution to the total number of negligible microspheres (N) is recorded as the spherical rate. The formula of the ball forming rate is as follows (3).

$$GR(\%) = \frac{N_2}{N} \times 100 \tag{3}$$

2.7. Morphology Observation and Particle Size Determination of Microspheres

Take appropriate amount of dried Bt microspheres to constant weight, and observe the surface morphology of the microspheres by SEM after spraying gold. To observe the internal structure of the microspheres, carefully cut the microspheres and observe their cross-sections. Randomly select a proper amount of prepared microspheres, measure the diameter of each sphere at three angles, prevent measurement inaccuracy caused by irregular microspheres, and calculate the average particle size of microspheres.

2.8. Release behavior of Bt microspheres

Take appropriate amount of Bt microspheres samples with biochar and without biochar in 100 mL sterilized distilled water (pH = 7.0 ± 0.2). Shaked at 120 rpm under 25 ℃, take 1 mL suspension every 1 hour, diluted a certain multiple, then cultured in PCA medium at 30 ± 1 ℃ for 24 h, recorded the number of colonies as the cumulative release amount (cfu · mL^{-1}) .

3. Results and discussion

### 3.1. Characterization of walnut shell biochar

Temperature is an important factor that determines the characteristics of biological properties. Biochar prepared at different temperatures has considerable differences in physical and chemical properties (Table 1). It can be seen that the yield, pH, and ash of biochar obtained from the walnut shell at 400, 500, and 600 ℃ were quite different.

Table 1. Physicochemical properties of walnut shell biochar.

	H-4	H-5	H-6
Yield (%)	35.98	31.10	25.33
pH	8.20	9.40	10.00
Ash content (%)	5.76	9.50	24.72

The yield of biochar is mainly affected by pyrolysis temperature, and the yield of biochar

decreases gradually with the increase of preparation temperature[21], while the ash content and pH increase with the increase of temperature. In general, biochar raw materials contain various plant acids, but the plant acids are gradually decomposed during pyrolysis, oxalate is mainly generated during low-temperature preparation, and carbonate is mainly generated during high-temperature preparation. Therefore, with the increase of temperature, the carbonate content gradually increases, increasing in pH value [22]. Therefore, biochar produced by plant straw can be used as a natural modifier for acidic soil [23].
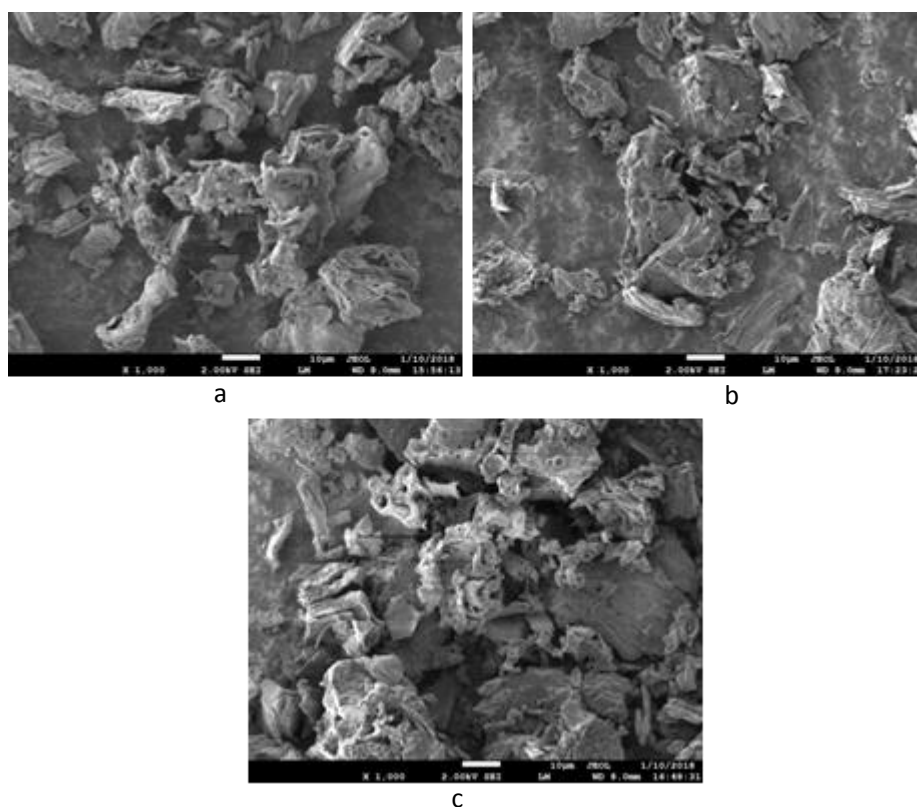
Fig. 1. Shows that SEM images of biochar were prepared at several different temperatures.
(a, b, c: 400, 500, 600 ℃)

It can be seen that the surface of biochar formed by pyrolysis of the walnut shell at different temperatures has an obvious pore structure, and the pore size and quantity of biochar are different. These pores are the important basis for the larger surface area and adsorption capacity of biochar [24], and also the main channel for Bt to enter the adsorbent. By comparing the biochar at 400 ℃, 500 ℃, and 600 ℃, we can see that the surface of biochar produced by pyrolysis of the walnut shell has a lot of pores, but the number of pore on the surface of biochar produced by pyrolysis at different temperatures is different, the average pore size of H-6 was greater than that of H-5 and H-4. Therefore, the variation trend of pore number and size increases with the increase of temperature.
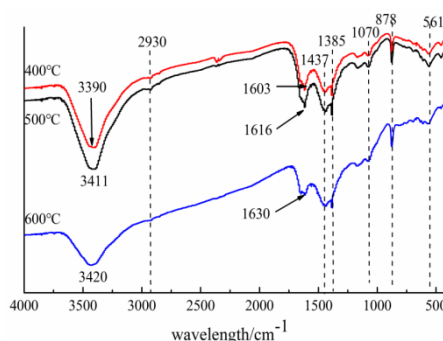
Fig. 2 FTIR spectra of biochar derived from different temperatures

The surface functional groups of walnut shell biochar prepared at different pyrolysis temperatures are different, as shown in Fig. 2 infrared spectra. The characteristic peaks of biochar are mainly absorption peaks of 3390 cm-1, 2930 cm-1, 1603 cm-1, 1437 cm-1, 1070 cm-1, 878 cm-1, 561 cm-1. The FTIR spectrum of walnut shell biochar showed peaks at 3390 cm-1 corresponding to the stretching vibration of -OH groups [25]. The absorption at 2930 cm-1 indicates the stretching vibration of C-H, with only a very weak absorption peak at 400-500 ℃. The absorption peak disappears at 600 ℃, and alkyl groups are missing with the increase of pyrolysis temperature, indicating that the aromatization degree of biochar gradually increases [26]. The 1600-1630 cm-1 region is the characteristic absorption region of the aromatic ring skeleton structure [27]. The absorption peak gradually increases in the temperature range of 400-500 ℃, indicating that its aromatization degree increases while its intensity decreases at 600 ℃. It may be that the aromatization degree of biochar increases with the increase of pyrolysis temperature, which indicates that biochar components have experienced excessive carbon, amorphous carbon, and composite carbon in categories with the change of temperature [28]. 1473 cm-1 is the C-H absorption peak of the aliphatic group and 1385 cm-1 is the in-plane bending vibration peak of C-H in -CH3. The absorption peaks of -C-O and O-CH3 in lignin are about 1070 cm-1 in the fingerprint region. It can be seen that the pyrolysis of biochar retains the structural characteristics of protoplasm [29]. There are strong peaks of aromatic compounds at 878 cm-1 in the fingerprint region, and the absorption values of peaks at 561 cm-1 are almost the same at different temperatures, indicating that they may contain the same functional group [30].

3.2. Biochar effects on Bt biocompatibility

To investigate the effect of walnut shell biochar on the biocompatibility of Bt, the growth diameter of the colony of bacterial was measured by adding biochar into the culture medium. As is shown in Fig. 3, the effects of different amounts of biochar pyrolyzed at different temperatures on the growth of Bt were different, but there was no significant difference in the colony diameter of Bt growth with or without biochar. With the increase of the amount of biochar added in the medium, the influence on the growth diameter of the Bt colony was firstly promoted and then inhibited. That means biochar had a positive effect on the growth and reproduction of Bt at low concentration, and the excessive amount of biochar added inhibited the growth of Bt. This may be alkaline with biochar, and the higher the concentration, the higher the pH value of the medium, which is not conducive to the growth of Bt.
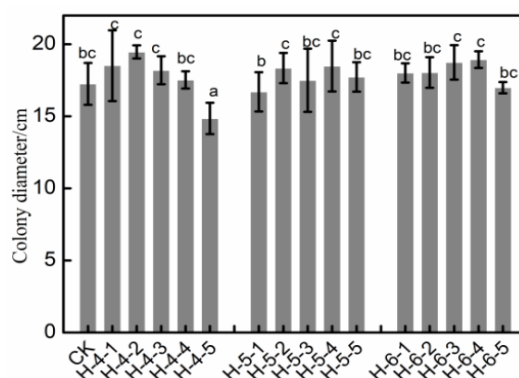
Fig. 3. Effect of biochar on the biocompatibility of Bt.

3.3. Process optimization

To obtain better conditions for microspheres preparation, the effects of sodium alginate concentration, CaCl2 concentration, and biochar addition amount on the embedding rate and granulation of microspheres were investigated. The effects of various factors on the embedding rate of microsphere are shown in Fig. 4.
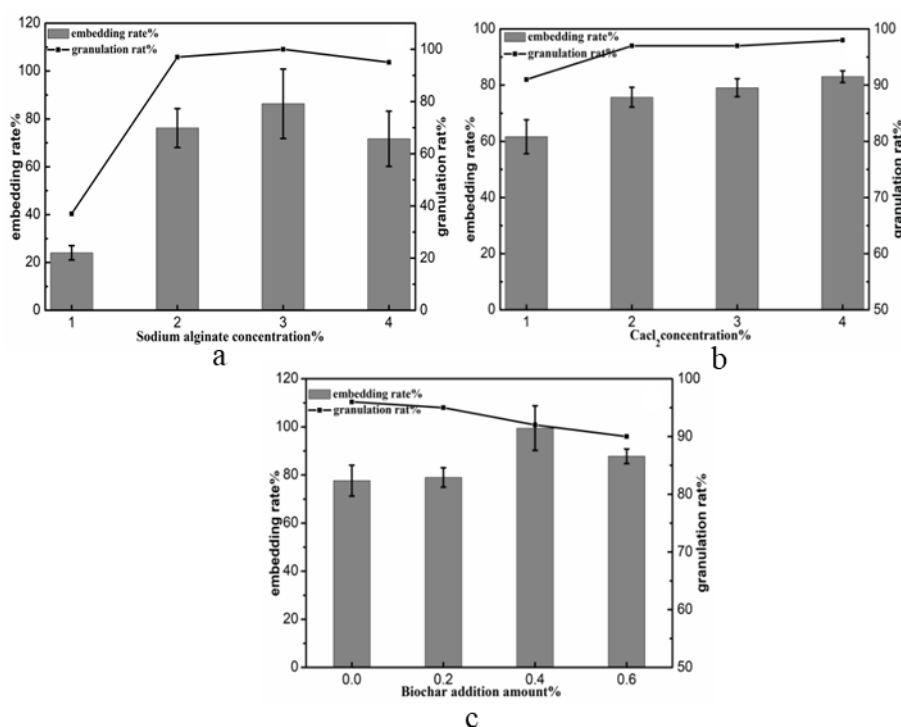

Fig. 4. Effects of variation of factors on embedding rate and granulating rate of Bt microspheres (a: Sodium alginate concentration; b: $CaCl_2$ concentration; c: Biochar addition amount).

Sodium alginate is used as the wall material of the microspheres, biochar is used as the adsorption material, calcium chloride is used as the cross-linking agent, all of which have different effects on the embedding rate and the forming rate of the microspheres. Fig. 4 (a) shows the effect of sodium alginate concentration on the embedding rate and granulation, when the mass fraction of

sodium alginate is 2 %- 4 %, the microsphere forming rate and embedding rate are both higher. The main reason is that when the mass fraction of sodium alginate is too low, the system formed by crosslinking with calcium chloride is loose in structure, poor in sphericity, and low in embedding rate [31]. However, in the experimental process, it is found that when the concentration of sodium alginate is too high, the viscosity of the solution increases, which will make it difficult to form microspheres, resulting in difficult granulation, low sphericity rate of microspheres, and uneven particle size. Fig. 4 (b) show the effect of $CaCl_2$ concentration on the embedding rate and granulation rate, When the mass fraction of calcium chloride is low, the exchange rate of Ca^{2+} and Na^+ in sodium alginate is low, and the weak curing action leads to low microsphere forming rate and embedding rate[32]; With the increase of calcium chloride concentration, the embedding rate and the forming rate of microspheres show an upward trend. However, the excessive concentration causes the crosslinking rate to be fast, the shape of the microspheres was irregular, and the hardness of the microspheres was too large, affect on the release of the core material [33]. Fig.4 (c) shows the effect of the biochar addition amount on the embedding rate and granulation. The addition of biochar can significantly improve the encapsulation rate of microspheres. At low concentration, the embedding rate of microspheres increases with the increase of biochar addition. However, at 0.6 % concentration, the exchange of Na^+ in sodium alginate solution and Ca^{2+} in calcium chloride solution may be hindered due to the excessive addition of biochar, and a tight network structure cannot be formed, which reduces the amount of Bt embedded in microspheres and is not conducive to droplet formation. To sum up, Bt microspheres were prepared with 3 % sodium alginate, 0.4 % biochar, and 2 % calcium chloride. The embedding rate and balling rate of microspheres are 93.50 % and 90 % respectively. The entrapment rate and balling rate of microspheres prepared under the same conditions without adding biochar were 80.33 % and 98.00 % respectively.

3.4. Characterization of Bt microspheres

Bt microspheres were prepared according to the optimal preparation conditions. The SEM morphologies of the two composite microspheres are shown in Fig. 5.
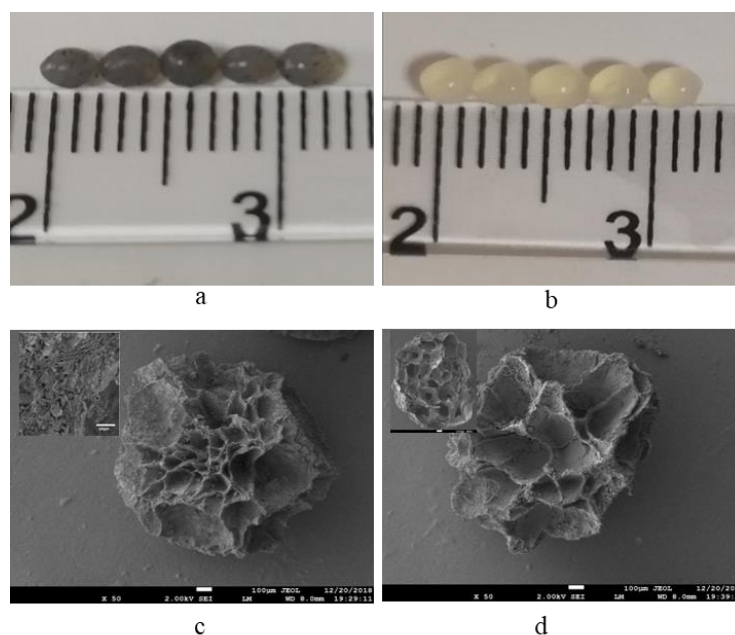

Fig. 5. Micrographs of microspheres (a, c: Bt-sodium alginate-biochar microspheres; b, d: Bt-sodium alginate microspheres).

As shown in Fig. 5, whether biochar is added or not, the two composite microspheres have good sphericity before drying, with a smooth, round surface and no tailing phenomenon. After drying, the surface of the microspheres presents many concavities and convexities, and holes, which is due to the water loss of the composite microspheres during the drying process, resulting in wrinkles on the surface of the spheres. There are a large number of interconnected pores in the microspheres with and without biochar, among which the microspheres with biochar are densely distributed and have small pore sizes, with the pore sizes ranging from 10 μm to 20 μm, and the particle sizes of the microspheres are about 1200 μm, while the microspheres without biochar are uniformly distributed and have slightly larger pore sizes, with the central pore sizes ranging from 50 μm to 100 μm and the particle sizes of the microspheres being about 1500 μm. The pores on the surface of the microspheres and the pores communicated inside the microspheres are important channels for the diffusion and release of embedded drugs [34].

3.5. Release behavior of Bt microspheres in water

As is shown in Fig. 6, the composite microspheres without biochar added had a faster release rate than the microspheres with biochar addition. At 96 h, the release curve tended to be stable, indicating that the Bt embedded in the microspheres was substantially completely released. Due to the addition of biochar, the microspheres have a tight internal structure and a large number of pores, which provides more space for adsorbing more Bt. Therefore, the microspheres added with biochar have a slow-release rate and a large cumulative release. The maximum was reached at 144h, after which the release profile showed a constant release tendency.
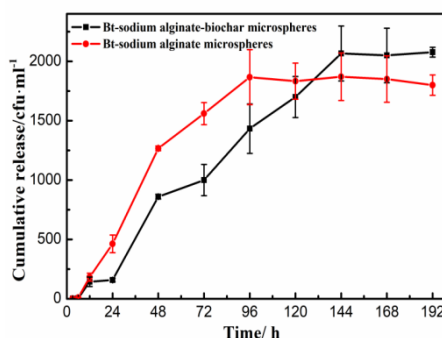

Fig. 6. Cumulative release of Bt microspheres in water.

4. Conclusions

Biochar was prepared by the pyrolysis of the walnut shell at different temperatures. Various biochars were characterized and analyzed. Biochar with good biocompatibility to Bt was screened out and added into microspheres as an adsorbent to improve the carrying capacity of core materials in microspheres. Taking Bt as the model drug, the embedding rate of Bt-sodium alginate-biochar composite microspheres was 93.50 % and the ball forming rate was 90 % by optimizing the preparation conditions under the conditions of 3 % sodium alginate, 2 % calcium chloride, and 0.4 % biochar addition. The release behavior of microspheres in water was studied. The results showed that adding biochar significantly improved the embedding rate of composite

microspheres and prolonged the release time of Bt in microspheres, which was of great significance to improve the persistence of the Bt sustained-release agent.

Acknowledgments

References

[1] M. Waqas, Y. H. Kim, A. L. Khan, R. Shahzad, S. Asaf, M. Hamayun, S. M. Kang, M. A. Khan, I. J. Lee, Journal of Zhejiang University Science B **18**(2), 109 (2017).

[2] J. Lehmann, M. C. Rillig, J. Thies, C. Masiello, W. Hockaday, D. Crowley, Soil Biology and Biochemistry **43**(9), 1812 (2011).

[3] N. Xu, G. C. Tan , H. Y. Wang, X. P. Gai, European Journal of Soil Biology **74**, 1 (2016).

[4] Y. X. Liu, L. Lonappan, S. K. Brar, S. M. Yang, Science of the total environment **645**, 60 (2018).

[5] Z. X. Tan, Y. H. Wang, A. Kasiuliene, C. Q. Huang, P. Ai, Clean Technologies and Environmental Policy **19**(3), 761 (2017).

[6] H. Y. Ji, Y. Y. Wang, H. H. Lyu, Y. X. Liu, R. Q. Yang, S. M. Yang, Chinese Journal of Applied Ecology **29**(4), 1328 (2018).

[7] S. I. Mulla , M. P. Talwar, Z. K. Bagewadi, R. S. Hoskeri, H. Z. Ninnekar, Chemosphere **90**(6), 1920 (2013).

[8] A. U. Rajapaksha, S. S. Chen, D. C. W. Tsang, M. Zhang, M. Vithanage, S. Mandal, B. Gao, N. S. Bolan, Y. S. Ok, Chemosphere **148**, 276 (2016).

[9] T. T. N. Nguyen, C. Y. Xu, I. Tahmasbian, Geoderma **288**, 79 (2017).

[10] L. Hale, M. Luth, D. Crowley, Soil Biology & Biochemistry **81**, 228 (2015).

[11] H. K. Askary, Biocontrol Science & Technology **24**(4), 462 (2014).

[12] R. Y. Wang, X. H. Fan, W. P. Cao, S. J. Ji, Acta phytophylacica sinica **2**, 223 (2003).

[13] Y. Zhang, G. L. Zheng, J. X. Tan, C. Y. Li, L. Y. Cheng, Microbiological Research **168**(8), 512517 (2013).

[14] C. T. Li, G. L. Zheng, Y. L. Yan, Authorized in January 2013. (P): 201110318767.5.

[15] X. J. Zhang, Screening of a highly UV resistant Bacillus thuringiensis mutant and optimize of its floating [D]. 2014.

[16] X. L. He, Z. Q. Sun, K. L. He, S. Y. Guo, Applied Microbiology and Biotechnology **101**(7), 2779 (2017).

[17] B. C. Josefina, V. C. Lucila, S. S. Dulce, P. L. G. Laura, S. F. Omar, Biocontrol Science and Technology **27**(1), 4257 (2017).

[18] S. Y. Tao, Z. S. Wu, X. F. He, B. C. Ye, C. Li, Bioresources **13**(1), 1773 (2018).

[19] M. Y. Qiu, K. Sun, J. Jin, B. Gao, Y. Yan, L .F. Han, F. C. Wu, B. S. Xing, Scientific Reports **4**, 5295 (2014).

[20] M. Carrier, A. G. Hardie, Ü. G. J. Uras, Journal of Analytical and Applied Pyrolysis **96**, 2432 (2010).

[21] M. Keiluweit, P. S. Nico, M. G. Johnson, M. Kleber, Environmental Science and Technology **44**, 12471253 (2010).

[22] J. Li, Physicochemical properties of different biochars and their adsorption on bisphenol A and sulfamethoxazole [D]. 2013.

[23] J. H. Yuan, R. K. Xu, H. Zhang, BioresourceTechnology **102**(3), 34883497 (2011).

[24] T. T. Wang, Z. S. Ren, X. L. Wang, J. Y. Zheng, Environmental Science &Technology **40**(1), 4248 (2017).

[25] F. Y. Li, J. G. Tao, J. F. Wang, Chinese Journal of Environmental Engineering **11**(6), 37263730 (2017).

[26] G. K. Parshetti, S. K. Hoekman, R. Balasubramanian, Bioresource Technology **135**, 683689 (2013).

[27] Q. F. Zheng, Y. H. Wang, Y. G. Sun, Spectroscopy and Spectral Analysis **4**, 962966 (2014).

[28] M. Keiluweit, P. S. Nico, M. G. Johnson, M. Kleber, Environmental Science and Technology **44**(4), 12471253 (2010).

[29] Y. Liu, X. Z. Yuan, H. J .Huang, X. L. Wang, H. Wang, G. M. Zeng, Fuel Processing Technology **112**(3), 93 (2013).

[30] P. L. Gim, Journal of Industrial and Engineering Chemistry **56**, 382393 (2017).

[31] S. J. Cheng, Q. N. Zhong, Y. Xie, China Pharmacist **16**(5), 658661 (2013).

[32] C. W. Liu, M.Y. Zeng, Z. F. Tong, T. Y. Wei, Chinese Traditional Patent Medicine **36**(3), 620622 (2014).

[33] Y. Liu, H. L. Zhou, L. Li, M. L. Ma , C. L. Wang , L. Zhang, J. J. Tan, Guangzhou Chemical Industry **43**(8), 6264 (2015).

[34] S. Y. Tao, Z. S. Wu, X. F. He, B. C. Ye, C. Li, Bioresources **13**(1), 17731786 (2018).